https://doi.org/10.5194/egusphere-2025-2539
Preprint. Discussion started: 1 September 2025

A New Hybrid Framework for Digital Terrain Modeling Using Sector-Based Neighbor Selection and Neural Network Blending

Kadir Akgol[1], Yelda Nur Kara[1]

[1]Civil Engineering Department, Giresun University, Giresun, 28200, Türkiye

Correspondence to: Kadir Akgol (kadirakgol@hotmail.com.tr)

Abstract. This paper presents a new hybrid framework for digital terrain modeling that combines directional sector-based neighbor selection (DSNS), artificial neural networks (ANN), and gradient-based weighted blending. The framework addresses the spatial imbalance and ripple artifacts commonly seen in interpolation-based terrain models. In the first stage, 12 sector-divided neighbors are selected around each query location to ensure directional balance. Next, ANN models are trained on reference terrains using either expert-adjusted or natural interpolated surfaces, depending on the test region. Finally, a gradient-based weighting mechanism blends ANN outputs with those of linear interpolation to create a coherent and smooth elevation surface. The proposed method is validated on three real-world terrains of varying size and complexity. Results show that the model significantly improves topographic continuity, numerical stability, and generalization across different landscapes. Compared to conventional interpolation methods, the proposed method reduces oscillations, maintains terrain flow, and eliminates the need for manual adjustments. The framework offers a scalable, automated, and accurate approach for terrain surface reconstruction in both regular and anisotropic datasets.

1 Introduction

Digital Terrain Models (DTMs) – often represented as gridded Digital Elevation Models (DEMs) – are fundamental in a wide range of engineering applications. They provide the basis for computing essential topographic attributes (e.g. slopes, watershed areas, volumes) that inform project planning and design (Çubukçu et al., 2022). In fields such as civil engineering, hydrology, and environmental management, accurate terrain models enable realistic simulations and analyses, from route alignment and earthwork calculations to flood risk assessment and drainage design (Mesa-Mingorance and Ariza-López, 2020). Consequently, the quality and accuracy of a DTM directly affect the reliability of any downstream analysis or decision. Researchers have noted that the overall *"quality of a DEM affects the results of its application"*, with vertical accuracy and resolution being especially critical (Abdel-Aziz et al., 2020). If a terrain model fails to capture important features (for instance, a sharp ridge or a deep channel), it can lead to misestimations – slopes and aspects might be computed incorrectly and volumes miscalculated – ultimately causing misinterpretations or poor engineering decisions (Rana, 2006; Darnell et al., 2010). High-precision DTMs are therefore not just a nicety but a necessity for ensuring the safety and efficiency of engineering projects.

https://doi.org/10.5194/egusphere-2025-2539
Preprint. Discussion started: 1 September 2025

Traditional approaches to DTM generation typically rely on well-established interpolation and triangulation algorithms implemented in GIS/CAD software (e.g. ArcGIS, NetCAD) or numerical computing environments like MATLAB. These methods use surveyed elevation points (from ground surveys or LiDAR) to interpolate a continuous surface. Common techniques include Triangulated Irregular Networks (TIN) based on Delaunay triangulation and grid interpolation methods such as Inverse Distance Weighting (IDW) or kriging (Fritsch et al., 1995; Baudot, 1991). Most widely used software packages default to TIN or IDW algorithms for DEM creation (Van Kreveld, 1996; Jiang et al., 2006). TIN models are popular due to their efficiency and ability to conform to irregular point distributions; a Delaunay-based TIN produces planar facets that exactly pass through the data points, requiring no complex tuning parameters (Ali and Mehrabian, 2009). This makes TIN interpolation a fast and robust choice for surface modeling in many cases. Likewise, deterministic interpolators like IDW are straightforward, averaging nearby point elevations with weights decreasing by distance, while kriging provides a geostatistical optimal estimation considering spatial autocorrelation. These conventional methods are relatively easy to implement and have proven reliable for generating DTMs under moderate conditions.

However, several limitations of the conventional DTM generation process are well recognized. Standard interpolation algorithms can struggle in complex terrain or heterogeneous land cover scenarios – for example, steep discontinuities (cliffs, embankments) or areas with non-ground objects (buildings, vegetation) often pose problems. Without additional constraints (such as breaklines) TIN models may oversimplify sharp features, and IDW or spline methods can introduce spurious "bumps" or depressions where data are sparse (Fan et al., 2014; Sakhaee and Entezari, 2015). Errors like overshoots, pits, and edge artifacts are common artifacts that require attention. In practice, it is often necessary for analysts to manually edit the generated surface to correct such issues: removing outlier points, enforcing known terrain breaklines, or locally re-interpolating problematic areas. Indeed, existing algorithms frequently *"fail in certain areas due to the complexity of scenes"* and *"extensive manual editing is required to obtain a clean representation of the ground surface in complex scenes"* (Hu and Tao, 2005; Florinsky, 2002). In urban or densely vegetated regions, for instance, automated filters might misclassify ground points, leaving errors that only expert intervention can fix. This manual post-processing not only consumes considerable time but also introduces subjectivity and inconsistencies. As a result, there is strong motivation to improve DTM generation workflows such that they yield high-accuracy models with minimal human intervention.

Improving the accuracy and automation of terrain modeling has been a focus of much recent research. On one hand, refinements to traditional techniques have been explored – for example, multi-resolution filtering and hierarchical algorithms can better distinguish ground terrain from off-terrain points (adapting to different terrain roughness levels) (Hu and Tao, 2005), and enforcing structural constraints (like ridge or drainage line enforcement) can make interpolated surfaces more realistic (Lindsay, 2016; Li et al., 2013). On the other hand, there is a clear trend toward data-driven methods that move beyond purely geometric interpolation. Modern "distribution-free" modeling techniques are being applied to DEM generation, including machine learning approaches that learn elevation patterns from data (Bandara et al., 2011). Notably, Artificial Neural Networks (ANNs) and other AI models have started to appear in the DEM literature as a means to capture complex nonlinear relationships in terrain data (Mesa-Mingorance and Ariza-López, 2020). For example, Bandara *et al.* used

https://doi.org/10.5194/egusphere-2025-2539
Preprint. Discussion started: 1 September 2025

an ANN to effectively *"project DSM data into DEM data"* in forested areas, demonstrating the potential of learning-based approaches to handle cases where few ground points are directly available (Bandara et al., 2011; Jiao and Liu, 2005). Similarly, fusing multiple sources or methods has proven beneficial; by combining the strengths of different DEM generation techniques, one can offset their individual weaknesses. A pertinent example is the fusion of InSAR-derived DEMs with optical-photogrammetry DEMs – since each data source has inherent limitations, their combination using neural networks was shown to produce a higher-quality elevation model than either alone (Gui et al., 2024; Zhang et al., 2016). Comparative studies in the literature underscore the value of such innovations. Çubukçu et al. (2022), for instance, evaluated ANN-based surface modeling against classical interpolators (IDW and kriging) for a river basin and found that while the ANN approach was viable, the kriging method yielded slightly better accuracy in their tests. This suggests that further improvements and hybrid approaches (integrating intelligence into the interpolation process) are needed for machine learning models to surpass the performance of well-established algorithms (Didona and Romano, 2015).

Given the importance of accuracy and the drawbacks of current methods, fully automating high-precision DTM generation remains an open challenge. As one study notes, generating a quality DTM still involves *"many problems that have to be solved"* with existing methods, and *"manual editing needs a lot of time,"* highlighting the need for more automated solutions (Bandara et al., 2011; Narendran et al., 2014). In this paper, we address this gap by presenting a novel terrain modeling approach that integrates a Directional Sector-Based Neighborhood Selection (DSNS) scheme with an artificial neural network for elevation estimation, followed by a weighted average blending of outputs. The proposed method is designed to reduce interpolation errors while minimizing manual intervention. In essence, the DSNS strategy divides the 360° surrounding of each interpolation location into angular sectors, ensuring that the algorithm selects representative reference points from all directions rather than relying solely on spatial proximity. These directionally-distributed neighbors (and combinations thereof) are then processed by an ANN which learns the relationship between local point configurations and the target elevation. Finally, a weighted averaging scheme blends the ANN outputs (potentially from multiple model realizations or sector combinations) to produce the final terrain elevation, lending additional stability and accuracy to the model. The key innovation of this approach is that it automates the neighbor selection and surface fitting process in an intelligent way, thereby greatly reducing the need for user tuning or corrections. The following sections of the paper detail the methodology and its implementation. We then compare the resulting DTM against surfaces generated by common software (NetCAD and MATLAB using standard interpolation algorithms) to evaluate performance gains. The results show that our method achieves higher accuracy with far less manual adjustment, underlining its potential as an efficient tool for digital terrain modeling in engineering projects.

https://doi.org/10.5194/egusphere-2025-2539
Preprint. Discussion started: 1 September 2025

2 Materials and Methods

2.1 Study Areas and Data Collection

In this study, three terrain regions located within the boundaries of Gümüşhane Province, Türkiye—namely Alemdar-1, Alemdar-2, and Hasanbey—were selected for experimental evaluation. These areas were chosen based on their varying topographic complexities and surface characteristics, which make them ideal candidates for testing terrain modeling accuracy and generalizability.

Alemdar-1, covering approximately 2,480 m², is situated along a narrow streambed and exhibits abrupt slope variations. Its complex morphology makes accurate terrain modeling particularly difficult. Detailed (X, Y, Z) coordinate data for this area were collected using GPS-based surveying methods. An initial surface model was created using NetCAD's Delaunay triangulation module, but it exhibited inconsistencies due to inappropriate triangle connections. As a result, expert-driven manual corrections were applied to refine the surface model. The revised model, visually validated against field conditions, was adopted as the internal reference surface for evaluating modeling performance at the Alemdar-1 site.

Alemdar-2 spans an area of 6,790 m² and exhibits a moderately sloped terrain characterized by smooth elevation transitions and regular contour flow. Compared to Alemdar-1, Alemdar-2 has a wider spatial extent and a more structured topographic pattern with fewer abrupt changes. These properties make it a suitable candidate for testing how well the proposed method maintains contour coherence in organized terrain settings. Its relatively uniform slope gradients and minimal localized irregularities allow focused evaluation of the interpolation quality without excessive surface noise. The terrain surface was modeled using automated workflows, providing a basis for testing the method's performance in cases where manual expert intervention is not present.

Hasanbey, the largest study area at 31,630 m², features a topographically more complex landscape than both Alemdar-1 and Alemdar-2. It includes a combination of smooth slope regions, artificial grading structures, and abrupt elevation shifts, making it representative of terrain scenarios often encountered in real-world infrastructure planning. This site was selected to test the scalability and adaptability of the proposed method across diverse micro-topographic features and varying slope intensities. The natural and structural heterogeneity of the area supports a comprehensive assessment of the model's ability to capture both gradual transitions and sharp terrain breaks without manual corrections.

All three areas are shown in Fig. 1, with contour samples and elevation maps later detailed in the results section. The integration of both expert-adjusted and unadjusted terrain surfaces across multiple regions enables a comprehensive evaluation of the proposed modeling techniques under varied real-world conditions. The datasets used for these evaluations, including both raw GPS measurements and grid-based models, are openly available via Figshare at https://doi.org/10.6084/m9.figshare.29279729.v1 (Akgol and Kara, 2025b).

https://doi.org/10.5194/egusphere-2025-2539
Preprint. Discussion started: 1 September 2025

Figure 1: Study area overview: Alemdar-1, Alemdar-2, and Hasanbey sites (© Google Earth 2025).

2.2 Proposed Three-Stage Terrain Modeling Framework

This study proposes a novel terrain modeling framework composed of three interconnected stages:

i. Directional Sector-Based Neighbor Selection (DSNS),
ii. Artificial Neural Network (ANN)-based elevation estimation, and
iii. Gradient-based Weighted Blending (GWB).

The proposed method is designed to mitigate interpolation errors caused by uneven point distributions or triangulation artifacts, while also minimizing the need for manual intervention—a challenge commonly reported in existing digital terrain modeling practices. The core principle is to intelligently guide the neighborhood selection, optimize elevation estimation using machine learning, and enhance surface smoothness through gradient-sensitive fusion. This integrative approach aims to address the limitations observed in both TIN-based models, such as those generated in NetCAD, and classic interpolation methods implemented in platforms like MATLAB.

A schematic overview of the proposed three-stage terrain modeling process is presented in Fig. 2, which outlines the data flow from raw (X, Y, Z) coordinates to the final digital terrain surface. First, the spatial domain around each grid point is divided into 30° angular sectors using the DSNS approach, and one representative point is selected from each sector. This

https://doi.org/10.5194/egusphere-2025-2539
Preprint. Discussion started: 1 September 2025

method ensures a directional balance in the selection of neighbor points, avoiding the pitfalls of proximity-only based selection seen in standard IDW or TIN implementations.

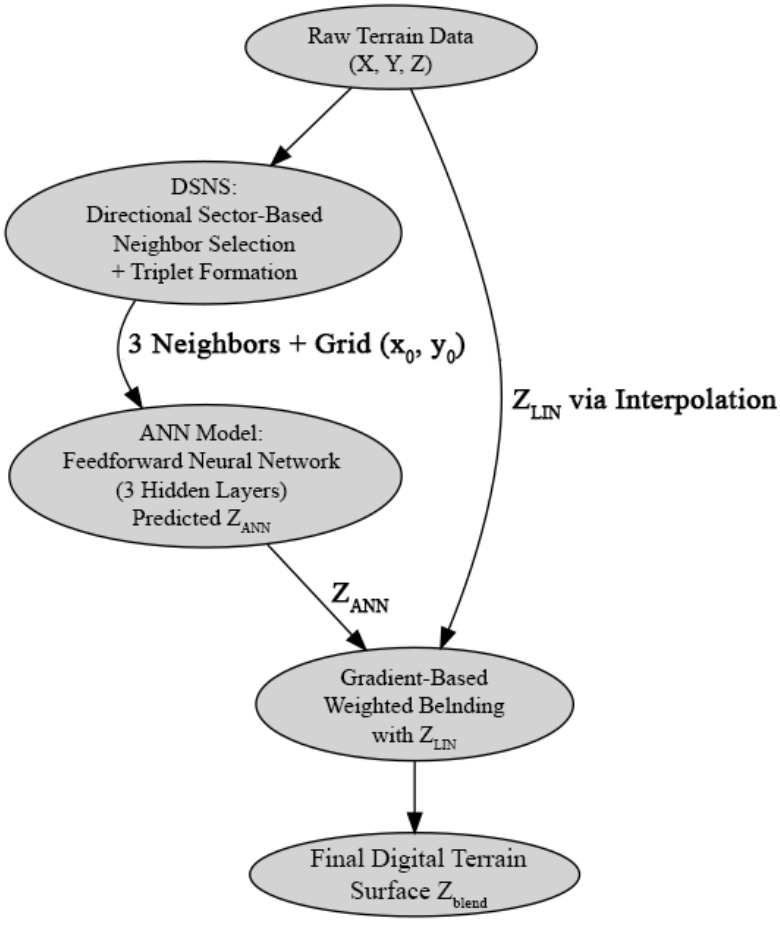

Figure 2: Workflow diagram of the proposed three-stage terrain modeling framework.

Next, ANN-based regression is used to estimate the elevation at the target grid point using geometric and altimetric features of the selected neighbors. While similar studies have explored ANN models for DEM post-processing or terrain prediction, their application has often been limited to fusing multi-source data or reclassifying elevation bands. In contrast, this study utilizes ANN directly for local, structure-aware surface generation.

Finally, a gradient-sensitive weighted blending stage fuses the ANN-predicted elevation values with those computed via classical linear interpolation. This step compensates for the local smoothness deficiencies of ANN and helps reduce surface discontinuities in steep terrain zones. Such hybrid approaches, though previously attempted in kriging-ANN fusion models, rarely implement gradient-based adaptive weighting, which is a distinctive contribution of this method.

Overall, the proposed methodology combines the geometrical coverage of sector-based neighbor selection, the non-linear learning capacity of neural networks, and the structural coherence of classical interpolators. As detailed in the following

https://doi.org/10.5194/egusphere-2025-2539
Preprint. Discussion started: 1 September 2025

subsections, this approach offers a promising balance between automation, accuracy, and surface continuity, particularly for terrain regions with complex topographic features.

2.2.1 Directional Sector-Based Neighbor Selection (DSNS)

In conventional interpolation methods, neighbor points are typically selected based solely on their Euclidean proximity to the query location. However, such approaches often result in spatial imbalance and fail to account for directional variability, especially in irregularly distributed terrain data. To overcome this limitation, we introduce the Directional Sector-Based Neighbor Selection (DSNS) strategy. This method partitions the 360° region surrounding a grid point into 12 equal angular sectors (30° each) and selects one representative reference point from each sector. This ensures a directionally balanced neighbor configuration. Figure 3 illustrates a practical example of the DSNS scheme, showing a grid layout with reference points, sector divisions, and selected neighbors.

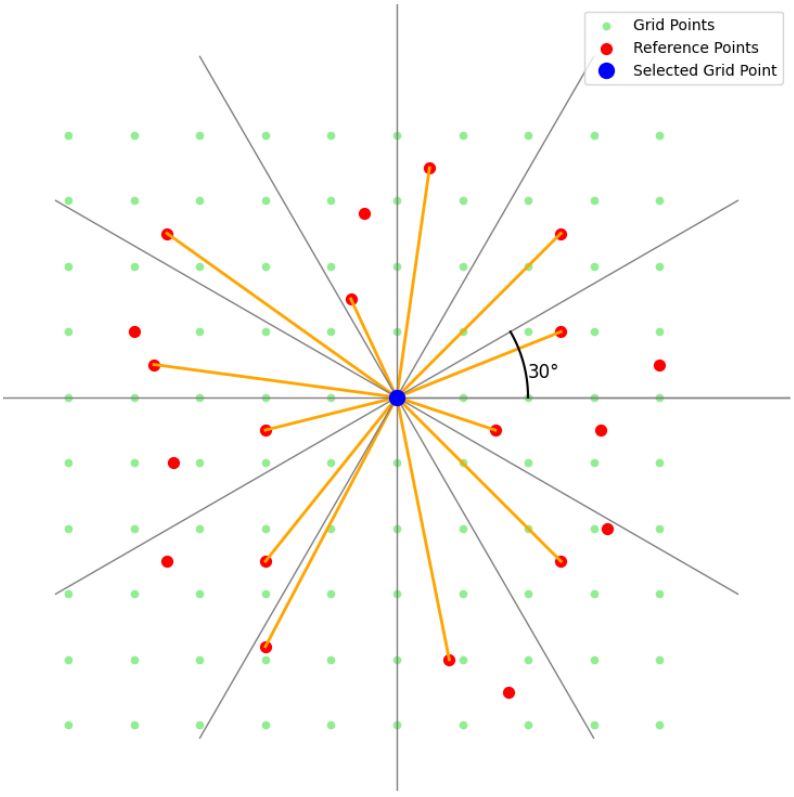

Figure 3: Directional Sector-Based Neighbor Selection (DSNS).

The selected grid point (blue) is centered within 12 equally spaced angular sectors (30° each). One reference point (red) is selected per sector based on proximity. Light green dots represent surrounding grid points; orange lines indicate the selected neighbors (Figure 3).

https://doi.org/10.5194/egusphere-2025-2539
Preprint. Discussion started: 1 September 2025

For each grid location $g = (x_0, y_0)$, the azimuth angle θ_i between the grid point and a reference candidate $p_i = (x_i, y_i)$ is computed using the two-argument arctangent function (Eq. 1).

$$\theta_i = atan2\,(y_i - y_0,\ x_i - x_0) \tag{1}$$

This angle, originally in radians, is converted to degrees and normalized to the [0°, 360°) interval (Eq. 2).

$$\theta_i° = \theta_i \cdot \frac{180}{\pi} + 180 \tag{2}$$

Based on the angular position, the corresponding sector index s_i is calculated as (Eq. 3).

$$s_i = \left\lfloor \frac{\theta_i°}{30} \right\rfloor + 1 \tag{3}$$

Within each sector, the closest point p_s to the grid point is selected according to its Euclidean distance (Eq. 4).

$$d_i = \sqrt{(x_i - x_0)^2 + (y_i - y_0)^2} \tag{4}$$

From the set of up to 12 selected points, all unique combinations of three points are considered. For each triplet (p_i, p_j, p_k), a centroid is computed (Eq. 5).

$$c_{ijk} = \frac{1}{3}\left[(x_i + x_j + x_k), (y_i + y_j + y_k), (z_i + z_j + z_k)\right] \tag{5}$$

To evaluate the geometric stability of each triplet, a selection score is defined as (Eq. 6).

$$S(i,j,k) = \left\|g - c_{ijk}\right\| \cdot (\|g - p_i\| + \|g - p_i\| + \|g - p_i\|) \tag{6}$$

The triplet with the minimum score is chosen as the optimal neighbor configuration for the grid location (Eq. 7).

$$(i^*, j^*, k^*) = \arg\min_{i,j,k} S\,(i,j,k) \tag{7}$$

To clarify the notation used above, the symbol $g = (x_0, y_0)$ refers to the interpolation or grid point at which the elevation is to be estimated. Each reference point is denoted as $p_i = (x_i, y_i, z_i)$, containing both positional and altimetric information. The azimuth angle θ_i represents the angle between the horizontal axis and the vector from the grid point to p_i, while s_i is the sector index that categorizes p_i based on its direction relative to g. The distance between the grid point and a reference point is represented by d_i. For any triplet of selected reference points, the centroid is defined as c_{ijk}, and the corresponding score function $S(i,j,k)$ quantifies the geometric suitability of the triplet based on its spatial arrangement relative to the grid point.

This directional selection mechanism ensures that the chosen reference points form a geometrically stable and spatially balanced base for surface estimation. It mitigates anisotropic clustering, reduces potential for degenerate triangle configurations, and provides robustness in complex terrains—issues commonly encountered in conventional triangulation and IDW-based systems (Stupariu, 2021).

https://doi.org/10.5194/egusphere-2025-2539
Preprint. Discussion started: 1 September 2025

2.2.2 Elevation Estimation via Artificial Neural Networks (ANN)

To accurately estimate terrain elevations from directionally balanced neighbor sets, an artificial neural network (ANN) architecture was developed and trained using the MATLAB Neural Network Toolbox. The network structure, input configuration, training parameters, and evaluation metrics were carefully selected to optimize performance on a moderately sized, structured dataset.

Each interpolation target point was associated with three reference points selected using the DSNS method. The coordinates (x, y, z) of these three points formed the first nine inputs. The remaining two inputs corresponded to the (x, y) coordinates of the target grid location. Consequently, each training instance was represented as an 11-element input vector (Eq. 8).

$$X = \left[x_1, y_1, z_1, x_2, y_2, z_2, x_3, y_3, z_3, x_g, y_g\right]^T \tag{8}$$

The target output for each input vector was the elevation z_g of the corresponding grid location, derived from expert-adjusted terrain models.

Prior to training, all input and output variables were normalized using min-max scaling, which linearly maps each feature to a [0, 1] interval based on its minimum and maximum values. This transformation improves numerical stability and supports faster convergence during backpropagation. The ANN architecture, visualized in Fig. 4, consists of three hidden layers, each comprising 10 neurons. All hidden layers employ the tangent-sigmoid (tansig) activation function, while the output layer uses a linear activation to map the learned features to the elevation estimate.

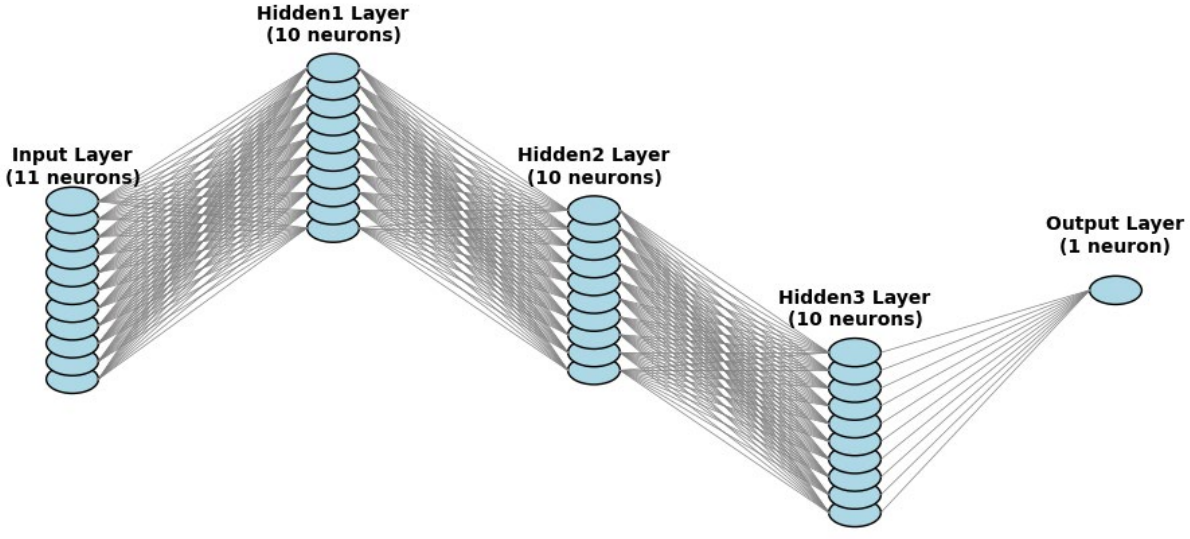

Figure 4: Architecture of the artificial neural network used for elevation estimation.

The network was trained using the Levenberg–Marquardt (LM) backpropagation algorithm, well-suited for moderate-sized regression problems due to its hybrid optimization capabilities combining gradient descent and second-order methods. The

https://doi.org/10.5194/egusphere-2025-2539
Preprint. Discussion started: 1 September 2025

dataset was randomly split into 70% for training, 15% for validation, and 15% for testing. Figure 5 and Table 1 present the overall training and validation performance of the ANN model used in the proposed terrain modeling framework.

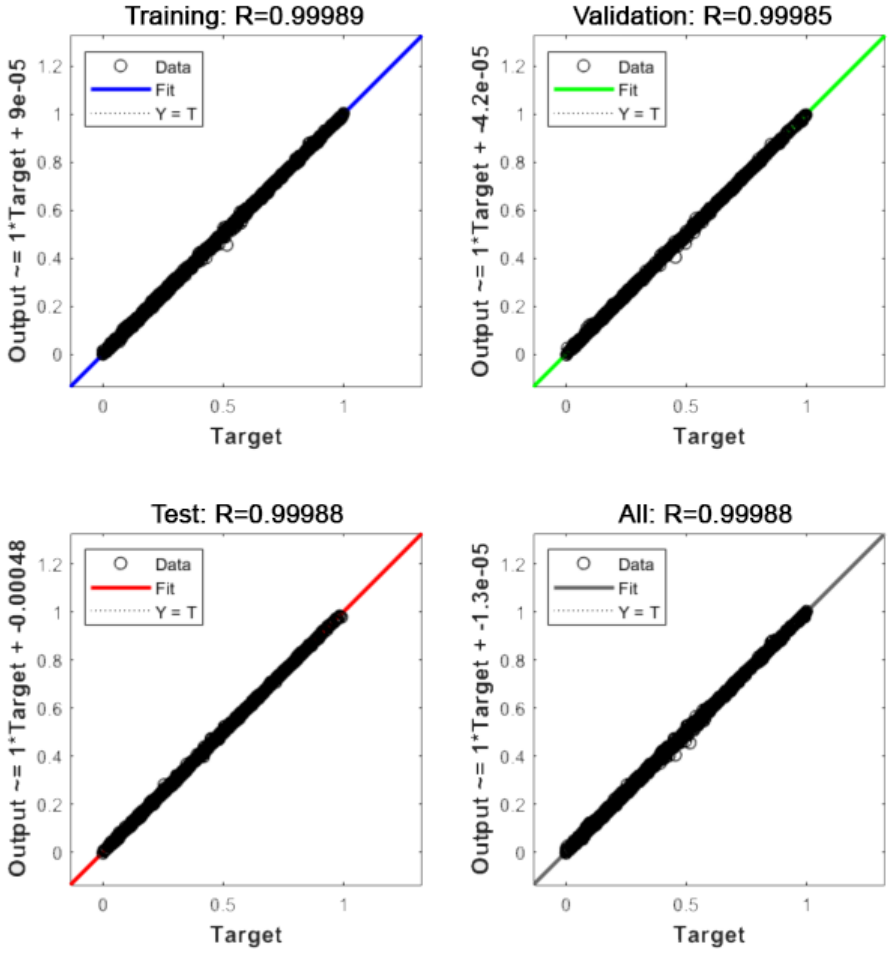

Figure 5: Regression performance plots for the training, validation, test, and all data sets.

Table 1: Summary of ANN hyperparameters and final performance metrics.

Unit	Initial Value	Stopped Value	Target Value
Epoch	0	704	1000
Elapsed Time	-	00:00:58	-
Performance	1.24	1.01E-05	0
Gradient	4.5	0.000136	1.00E-07
Mu	0.001	1.00E-09	1.00E+10
Validation Checks	0	6	6

https://doi.org/10.5194/egusphere-2025-2539
Preprint. Discussion started: 1 September 2025

The training process converged after 704 epochs, well before the upper limit of 1000, indicating fast and stable convergence behavior. The final mean squared error (MSE) was 1.01×10^{-5}, demonstrating high numerical accuracy across the dataset. Regression coefficients (R) were recorded as 0.99989 for training, 0.99985 for validation, and 0.99988 for testing subsets, with an overall correlation of 0.99988. These values confirm the ANN's robust generalization capability and absence of overfitting. After training, all predicted outputs were rescaled to their original elevation values using the inverse of the min-max normalization transformation. These rescaled predictions were subsequently used in the final blending stage of the proposed terrain modeling framework.

2.2.3 Gradient-Based Weighted Average Blending (GWB)

To generate a smoother and more accurate terrain surface, this study proposes a gradient-based weighted average blending method that combines the strengths of both the Artificial Neural Network (ANN) and the linear interpolation results. While the ANN-based model offers high prediction accuracy, it may introduce local artifacts such as sharp contour transitions due to overfitting in sparse regions. Conversely, the linear interpolation method provides smoother transitions but often lacks local accuracy. By integrating these two methods using a gradient-informed weighting scheme, both accuracy and surface smoothness can be achieved simultaneously.

The effectiveness of blending multiple models to improve prediction reliability and reduce model-specific biases has been demonstrated in various domains. For instance, Besic et al. (2025) Besic et al. (2025) utilized Bayesian model averaging to combine different remote-sensing-based forest canopy height models, showing that such fusion provides a more comprehensive representation of spatial uncertainty and mitigates the individual limitations of each model. Likewise, Li et al. (2023) Li et al. (2024) applied multi-task deep learning and data fusion strategies to extract building height and footprint from satellite imagery, highlighting that the integration of multiple information sources and model outputs leads to superior accuracy, especially in complex urban landscapes. In the context of digital terrain modeling, our blending approach serves a similar function: it synthesizes the complementary strengths of machine learning and classical interpolation, resulting in elevation surfaces that better capture both global landform structure and local detail.

Gradient magnitude is a measure of surface steepness and is computed from the elevation matrices of each method. Areas with high gradients typically correspond to sharp, unnatural contour bends which are undesirable in terrain models. Therefore, regions with lower gradients are considered to offer more reliable and realistic transitions. In this context, the blending weights are defined inversely proportional to the gradient magnitude (Eq. 9, 10).

$$G_{ANN}(i,j) = \sqrt{\left(\frac{\partial Z_{ANN}}{\partial x}\right)^2 + \left(\frac{\partial Z_{ANN}}{\partial y}\right)^2} \tag{9}$$

$$G_{LIN}(i,j) = \sqrt{\left(\frac{\partial Z_{LIN}}{\partial x}\right)^2 + \left(\frac{\partial Z_{LIN}}{\partial y}\right)^2} \tag{10}$$

https://doi.org/10.5194/egusphere-2025-2539
Preprint. Discussion started: 1 September 2025

where Z_{ANN} (previously denoted as z_g) and Z_{LIN} are the elevation matrices derived from the ANN model and the linear interpolation method, respectively.

The unnormalized weights are then computed as (Eq. 11, 12).

$$w'_{ANN}(i,j) = \frac{1}{1 + G_{ANN}(i,j)} \tag{11}$$

$$w'_{LIN}(i,j) = \frac{1}{1 + G_{LIN}(i,j)} \tag{12}$$

These are normalized to ensure they sum to one (Eq. 13, 14).

$$w_{ANN}(i,j) = \frac{w'_{ANN}(i,j)}{w'_{ANN}(i,j) + w'_{ANN}(i,j)} \tag{13}$$

$$w_{LIN}(i,j) = 1 - w_{ANN}(i,j) \tag{14}$$

The final blended elevation at each grid location is then calculated using a weighted average of both methods (Eq. 15).

$$Z_{blend}(i,j) = w_{ANN}(i,j) \cdot Z_{ANN}(i,j) + w_{LIN}(i,j) \cdot Z_{LIN}(i,j) \tag{15}$$

This approach ensures that smoother surfaces from the linear model are favored where appropriate, while high-accuracy predictions from the ANN model are retained in less variable regions. This blending step is also reflected in the final stage of the overall modeling workflow shown previously in Fig. 2, where gradient analysis and weight normalization are integrated to produce the final terrain surface.

The entire proposed modeling framework—including directional neighbor selection, ANN-based elevation estimation, gradient-based blending, and contour visualization—was implemented in MATLAB as a fully automated workflow. Through the integration of min-max normalization procedures, pre-trained neural networks, and built-in interpolation and plotting functions, the system requires no manual intervention once the initial terrain data are loaded. This automation ensures reproducibility, reduces user-induced variability, and enables rapid surface generation across diverse terrain datasets.

3 Results and Discussion

3.1 Comparative Analysis of Neighbor Selection Methods

To illustrate the structural differences in neighbor selection strategies, a synthetic test case was constructed using a grid point at the origin and 20 randomly distributed reference points within a 4×4 m² area. This setup mimics typical local terrain data distributions with varying densities and angular gaps. The aim was to visualize how different methods select neighboring points and how well they distribute these selections across the 360° directional space. Four commonly used strategies were examined: Nearest Neighbor (k=3), TIN-style selection (6 closest points), Voronoi-like selection (all surrounding points),

https://doi.org/10.5194/egusphere-2025-2539
Preprint. Discussion started: 1 September 2025

and the proposed DSNS method with 12 angular sectors. Each method's selected neighbors were visualized, and the corresponding angular distributions were analyzed (Figure 6).

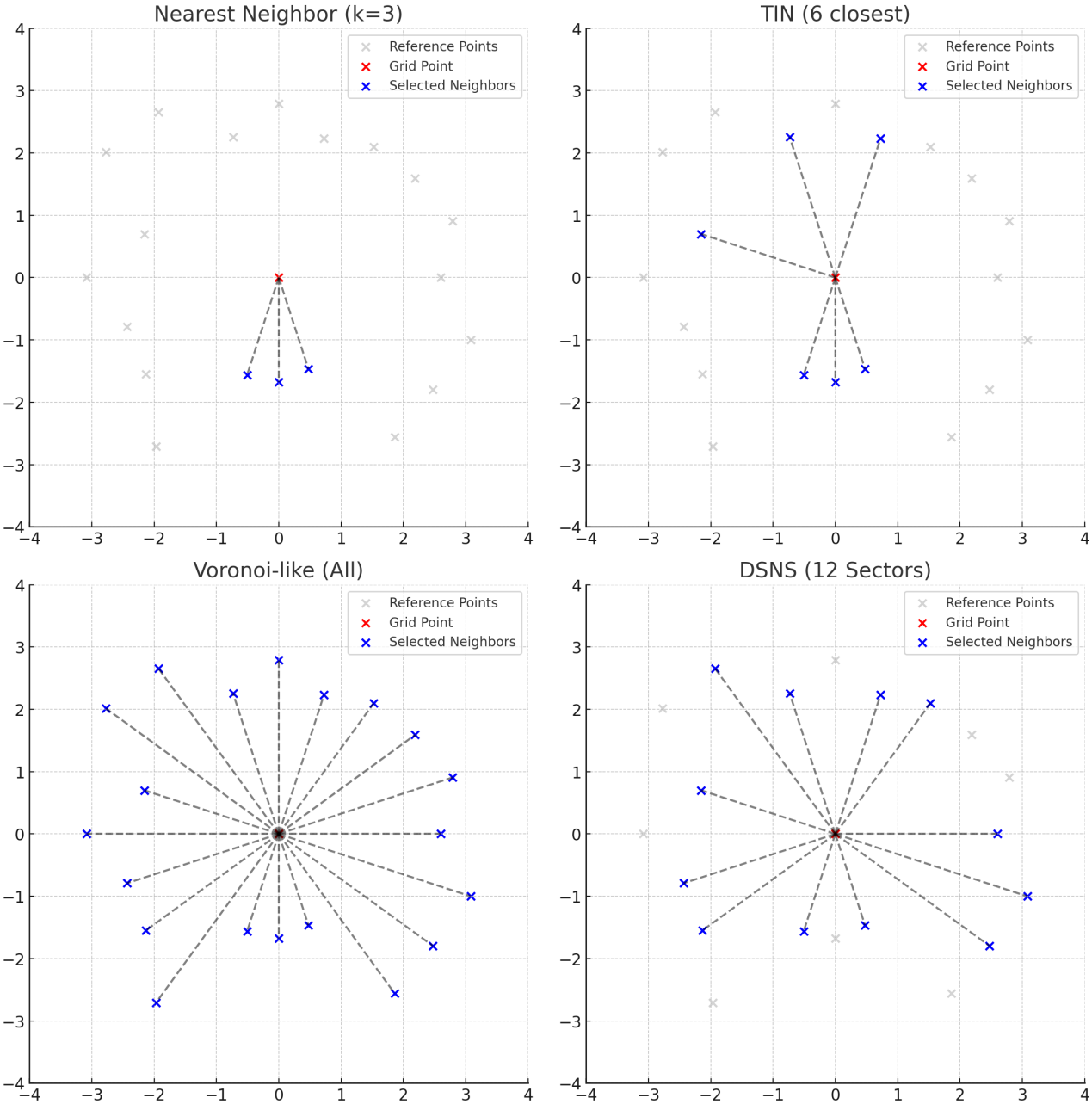

Figure 6: Directional distribution of selected neighbors using four different selection methods.

For each method, the polar angle (in degrees) between the grid point and its selected neighbors was computed. The angles were sorted to identify the mean and maximum angular gaps between consecutive neighbors. Additionally, a 12-sector radial

https://doi.org/10.5194/egusphere-2025-2539
Preprint. Discussion started: 1 September 2025

coverage scheme was used to calculate the percentage of the circle that was effectively covered (coverage ratio) and to estimate directional redundancy, defined as the average number of neighbors per occupied sector. These metrics are summarized in Table 2 and provide a quantitative basis for comparing directional diversity and spatial balance among the different selection approaches.

Table 2: Quantitative comparison of angular coverage metrics across neighbor selection strategies.

	Mean Angular Gap (°)	Max Angular Gap (°)	Coverage Ratio (°)	Redundancy Index
Nearest Neighbor	120.0	324.0	16.7	1.50
TIN	60.0	144.0	41.7	1.20
Voronoi-like	18.0	18.0	100.0	1.67
DSNS	30.0	54.0	100.0	1.00

As shown in Table 2, the proposed DSNS method demonstrates a well-balanced angular distribution, achieving full directional coverage (100%) and a redundancy index of 1.0—indicating that each sector is uniquely populated without excessive overlap. The method also achieves a mean angular gap of 30.0° and a maximum gap of 54.0°, reflecting a uniform spread of neighbors. In contrast, the Nearest Neighbor and TIN strategies result in significantly poorer angular coverage, with coverage ratios of only 16.7% and 41.7%, and maximum angular gaps of 324.0° and 144.0°, respectively. These large gaps highlight the risk of directional bias and underrepresentation in certain sectors. While the Voronoi-like method achieves 100% coverage, it suffers from a higher redundancy index (1.67), indicating that multiple neighbors fall within the same angular sectors, potentially introducing unnecessary computational overhead. These results confirm that DSNS provides a more efficient and geometrically diverse sampling of neighbors—crucial for improving spatial generalization in data-driven terrain modeling frameworks.

3.2 Validation of the Proposed Method on Alemdar-1

To evaluate the accuracy and practical effectiveness of the proposed terrain modeling method, a detailed performance comparison was conducted using the Alemdar-1 site, where an expert-validated reference model was available. Four different modeling approaches were tested: NetCAD's triangulated model (uncorrected), MATLAB's linear and natural neighbor interpolations, and the proposed ANN-based blended model. The comparative analysis and contour map visualizations were performed using custom MATLAB scripts developed for this study and made publicly available at https://doi.org/10.6084/m9.figshare.29279717.v1 (Akgol and Kara, 2025a).

Quantitative performance metrics—Root Mean Square Error (RMSE), Mean Absolute Error (MAE), and the coefficient of determination (R^2)—were calculated by comparing the estimated elevation values from each method against the reference model. The results are summarized in Table 3.

https://doi.org/10.5194/egusphere-2025-2539
Preprint. Discussion started: 1 September 2025

Table 3: Accuracy metrics for the Alemdar-1 site using different terrain modeling methods.

Metric	NetCAD	MATLAB Linear	MATLAB Natural	Proposed (ANN + Blending)
RMSE	0.14382	0.08969	0.19376	0.12187
MAE	0.02316	0.00879	0.10246	0.06664
R^2	0.99927	0.99971	0.99867	0.99948

As shown in Table 3, the proposed ANN + Blending method achieved a determination coefficient of $R^2 = 0.99948$, closely matching the highest value among all methods. Although MATLAB's linear interpolation method yielded slightly lower RMSE and MAE values, this improvement comes with a trade-off: it tends to over-smooth terrain features, reducing its ability to adapt to local irregularities and complex landforms. In contrast, the proposed method balances numerical accuracy with topographic realism by integrating the adaptability of machine learning with the continuity of classical interpolation. The NetCAD model exhibited higher RMSE and similar MAE compared to the proposed method, reinforcing the need for expert adjustments in its default output. Natural neighbor interpolation produced the highest RMSE and MAE, highlighting its limitations in steep or morphologically complex regions.

To further explore spatial behavior, Figure 7 presents contour maps for each method. The visual comparison highlights that the proposed method produces contour lines that are both smooth and aligned with natural terrain flow, closely matching the expert-validated surface. In contrast, the NetCAD and MATLAB natural outputs display irregular or distorted contours in sloped regions, while MATLAB linear interpolation, although smoother, oversimplifies the terrain in areas with high variability.

https://doi.org/10.5194/egusphere-2025-2539
Preprint. Discussion started: 1 September 2025

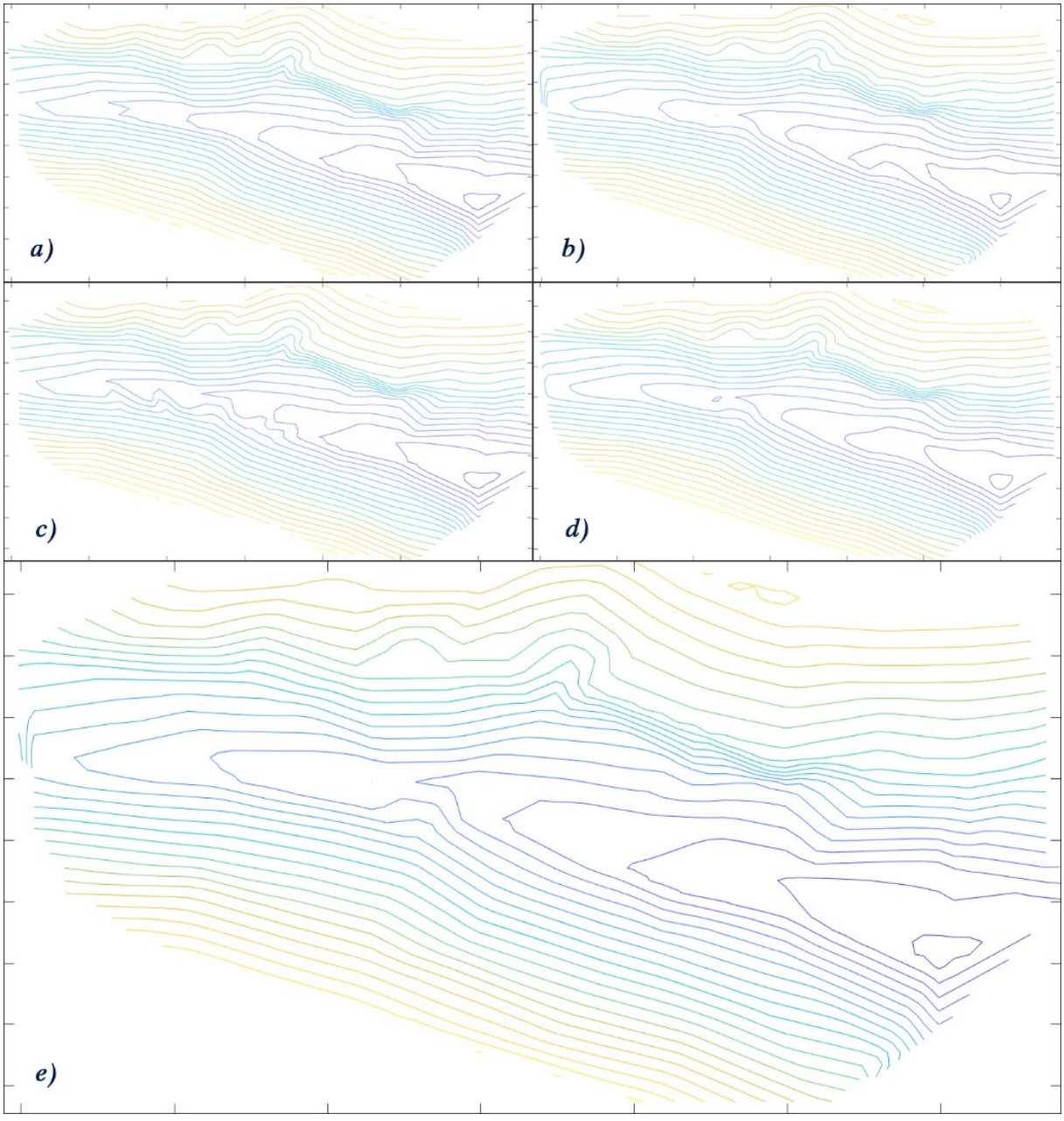

Figure 7: Comparative contour maps: (a) MATLAB Linear, (b) MATLAB Natural, (c) NetCAD uncorrected, (d) Proposed blended, (e) Reference terrain model.

The local accuracy of each model was further evaluated using absolute elevation difference maps, shown in Fig. 8. These maps visualize the pointwise elevation differences between the reference model and the outputs of each tested method. The colormap illustrates deviations from −1.5 meters to +1.5 meters, with warm tones indicating overestimation and cool tones indicating underestimation.

https://doi.org/10.5194/egusphere-2025-2539
Preprint. Discussion started: 1 September 2025

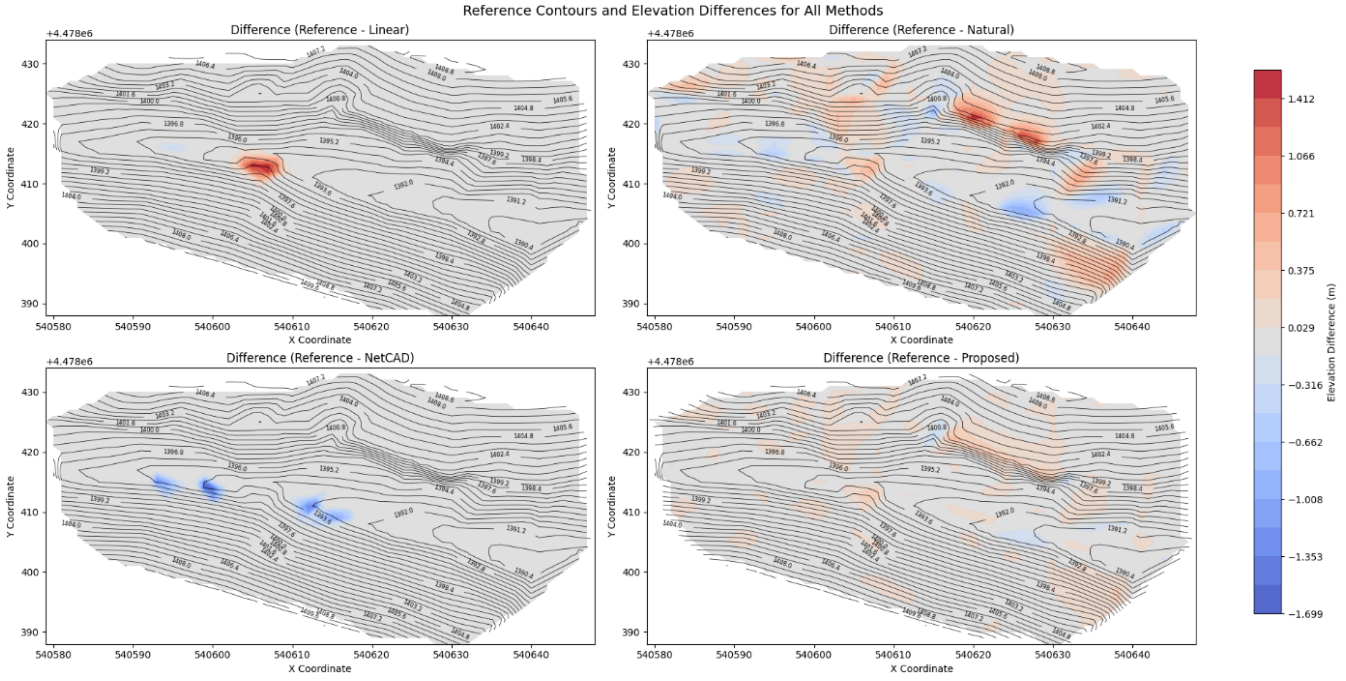

Figure 8: Absolute elevation difference maps with respect to the reference terrain for MATLAB linear interpolation, MATLAB natural interpolation, NetCAD uncorrected model, and Proposed ANN + Blending method.

As evident in the figure, the MATLAB Natural and NetCAD models exhibit noticeable localized deviations, particularly in areas with complex terrain morphology. The MATLAB Linear method shows very few but sharp discrepancies, especially near transition zones. In contrast, the proposed ANN + Blending method results in a more uniformly distributed error pattern with lower overall deviation magnitudes, confirming its robustness and spatial consistency across the modeling domain.

3.3 Validation on Alemdar-2: Slope-Sensitive Mid-Scale Site

To assess the consistency and robustness of the proposed terrain modeling framework, a second test was conducted on the Alemdar-2 site. This area, covering approximately 6,790 m², is located near a streambed and features sharp slope transitions within a relatively compact spatial domain. These characteristics make it an ideal case to evaluate how the model performs in high-gradient micro-environments. Despite the geometric and topographic differences from the Alemdar-1 site, the proposed ANN + Blending method maintained a high level of accuracy. A root means square error (RMSE) of 1.67×10^{-5} was achieved when compared to the expert-corrected reference model, underscoring the method's strong generalizability and numerical stability across varying terrain structures.

The contour map generated using the proposed method for this site is shown in Fig. 9. As evident in the figure, the contour lines are smooth, continuous, and free from artificial distortions, especially in slope transition zones adjacent to the stream. Unlike traditional interpolation techniques that tend to produce ripple effects or abrupt curvature changes in steep areas, the proposed method delivers a topographically coherent surface that aligns with expected terrain flow.

https://doi.org/10.5194/egusphere-2025-2539
Preprint. Discussion started: 1 September 2025

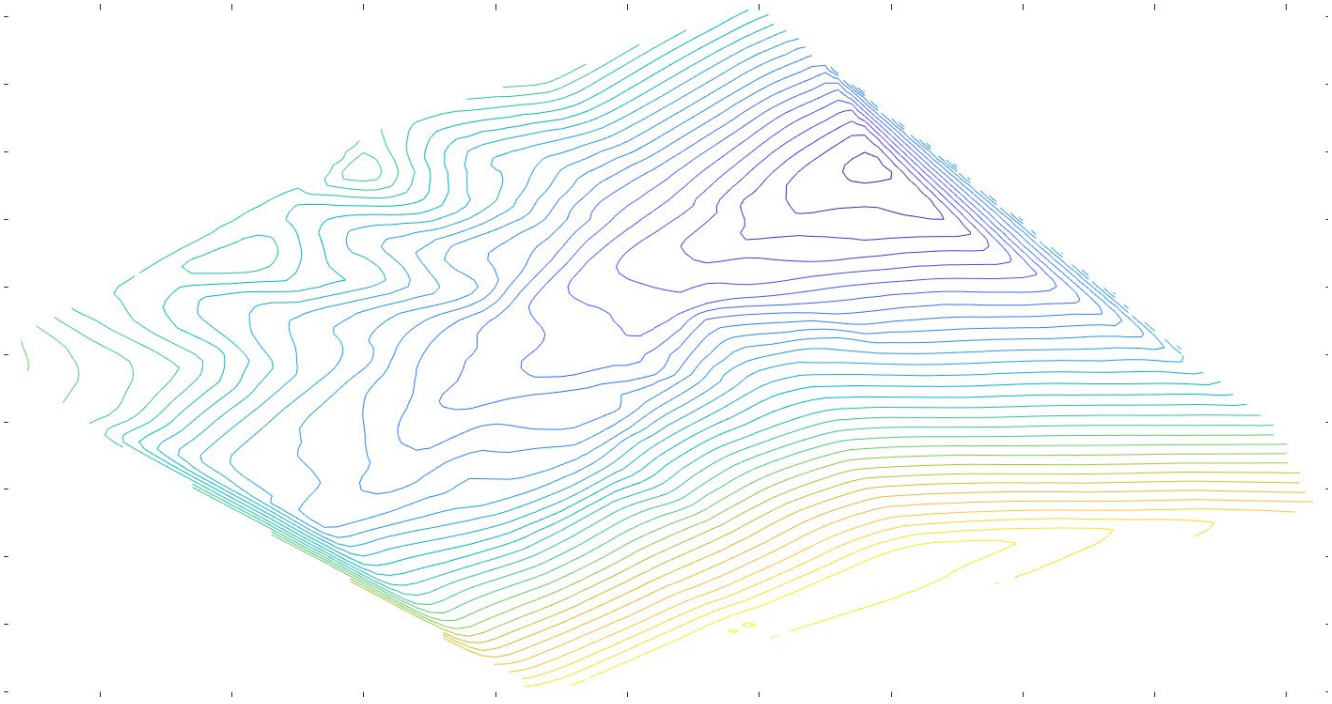

Figure 9: Contour map of the Alemdar-2 site generated using the proposed ANN + Blending method.

These findings demonstrate that the proposed approach excels in preserving terrain fidelity in slope-sensitive environments without requiring any manual intervention.

3.4 Validation on Hasanbey: Large-Scale Heterogeneous Terrain

The Hasanbey site, spanning approximately 31,630 m², represents the largest and most topographically diverse area in this study. This region contains a mix of smooth and abrupt terrain transitions, as well as localized elevation variations, making it particularly suitable for assessing the adaptability of terrain modeling techniques. As in previous analyses, the expert-adjusted TIN surface created in NetCAD is used as the reference model to evaluate the comparative performance of interpolation-based and learning-based methods.

To further validate the robustness of the proposed ANN + Blending approach, it was applied to this large-scale region and compared against MATLAB's linear and natural neighbor interpolations. Figure 10 presents the contour maps of the expert-adjusted reference model (left) and the proposed model (right). The proposed surface captures the overall landform continuity and ridge alignment effectively, producing smoother and more natural transitions across elevation zones.

https://doi.org/10.5194/egusphere-2025-2539
Preprint. Discussion started: 1 September 2025

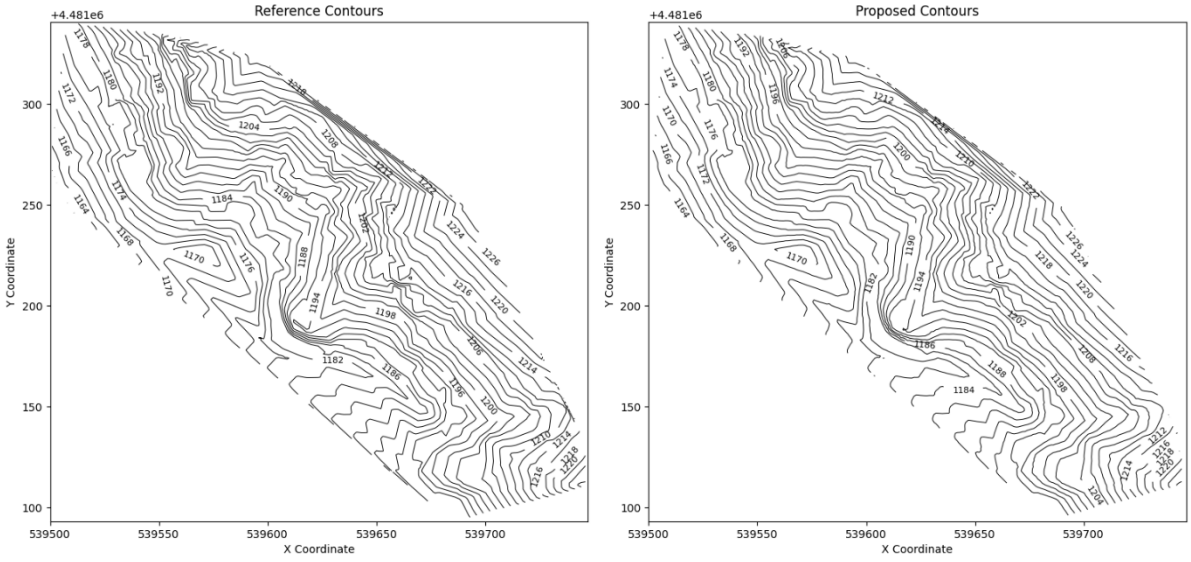

Figure 10: Contour maps for the Hasanbey site: Expert-adjusted reference model, Proposed ANN + Blending model.

In order to explore localized modeling discrepancies, the elevation differences between each method and the reference model were visualized in Fig. 11. These difference maps were superimposed with the contour lines of the reference surface to provide clearer spatial context.

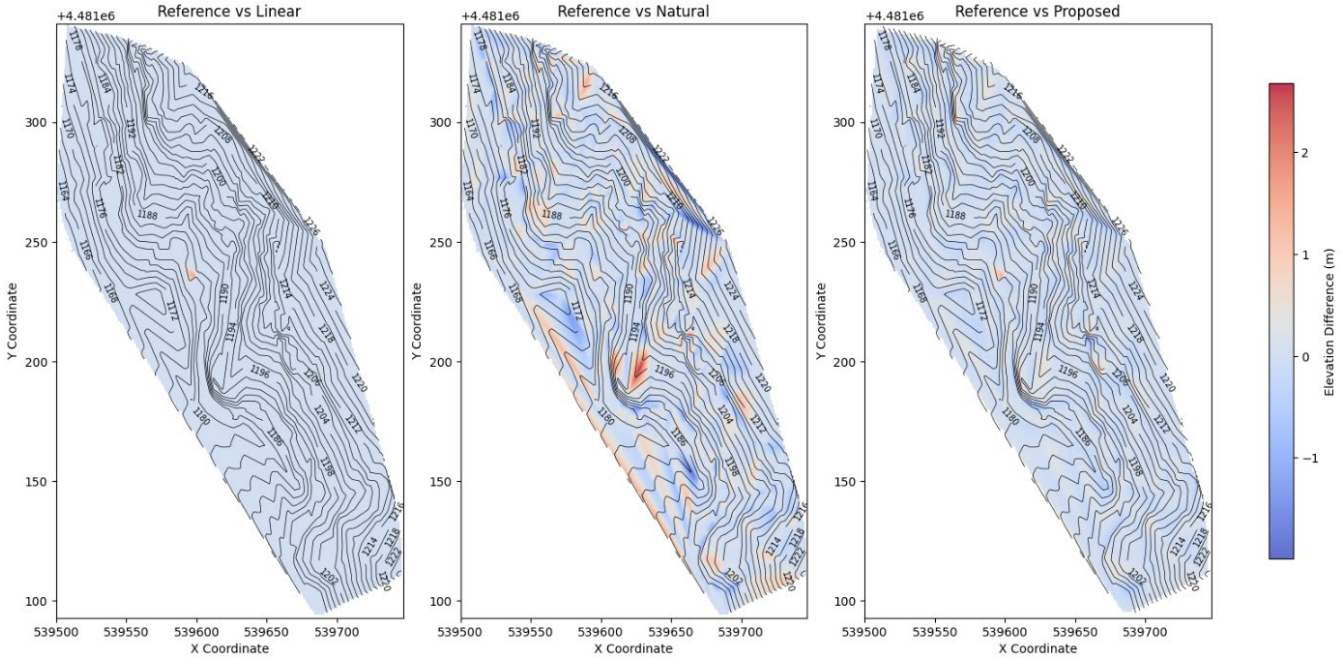

Figure 11: Elevation difference overlays with respect to the reference model: Reference vs. Linear, Reference vs. Natural, Reference vs. Proposed. Color gradients represent vertical deviations (in meters), with contour lines from the reference model overlaid for context.

https://doi.org/10.5194/egusphere-2025-2539
Preprint. Discussion started: 1 September 2025

The Reference vs. Linear comparison (left panel) shows systematic underestimations near slope breaklines, particularly around X = 539600–539610 and Y = 230–250. These artifacts stem from the angular nature of the linear method, which often fails to represent continuous terrain transitions accurately. In the Reference vs. Natural comparison (middle panel), deviations appear more irregular and oscillatory, introducing artificial features such as local ridges and valleys—especially in the central and southeastern zones. These are evident in scattered red and blue patches misaligned with the reference contour flow. In contrast, the Reference vs. Proposed panel (right) displays minimal deviation across the study area. Most differences remain within ±0.5 m and closely follow the terrain structure, indicating that the proposed method achieves both numerical precision and topographic realism more effectively than the interpolation-based techniques.

The mean squared error (MSE) of the proposed model for this site was calculated as 4.116×10^{-5}, confirming the method's scalability and precision even on extensive and complex terrain. While the reference surface required manual correction to eliminate geometric inconsistencies in the TIN network, the proposed approach achieved a comparable or better result through a fully automated process. These results demonstrate that the proposed model balances local detail and regional terrain continuity, achieving reliable results without manual corrections.

4 Conclusion

The comparative results (Figures 10 and 11) highlight that the proposed ANN + Blending model produces a markedly smoother and more continuous terrain surface relative to traditional interpolation methods. In the elevation difference overlays of Figure 11, the ANN-based approach exhibits diffuse, "fuzzy" color regions – an indication that deviations from the reference TIN surface are minor in magnitude and gradually varying spatially, rather than abrupt. By contrast, the MATLAB linear interpolation yields sharper, more localized discrepancies; for example, systematic underestimations appear along slope breaklines, suggesting that the linear method imposes angular, segmented transitions on the terrain (Arun, 2013). Similarly, while MATLAB's natural neighbor interpolation produces smoother transitions than linear overall, it introduces oscillatory artifacts – spurious small ridges and depressions that cut across the reference contours in an unrealistic manner (Bertram and Hagen, 2009). In stark difference, the ANN + Blending model avoids these issues: its discrepancies remain largely within a narrow ±0.5 m band and they align closely with the terrain's true contour structure. This indicates that our approach not only achieves high point-wise accuracy, but also preserves the continuity of landform features more faithfully than the conventional methods.

These visually smoothed transitions in the ANN-based model likely reflect a more realistic representation of the terrain's continuous nature. Real landscapes (except at genuine discontinuities like cliffs) tend to change elevation gradually, with smooth curvatures that are difficult to capture using planar facets alone (Heimsath and Farid, 2002). In contrast, a triangulated irregular network, even when expertly constructed, is inherently constrained to piecewise-planar facets between data points (Alavi et al., 1987; Eurich and Schulzke, 2004; Bertram et al., 2000). This means that a TIN may inadvertently introduce subtle artificial slope breaks or flat patches where the actual terrain has gentle curvature (Rebecca and Gold, 2004;

https://doi.org/10.5194/egusphere-2025-2539
Preprint. Discussion started: 1 September 2025

Magillo et al., 2013; Li and Kuai, 2014). Indeed, without additional constraints such as breaklines, TIN models are known to oversimplify sharp or curved features (Jiang and Xie, 2005; Ali and Mehrabian, 2009). The reference surface in this study was an expert-adjusted TIN, chosen for its overall accuracy; however, the sharper deviations seen in the linear interpolation's difference map and the unnatural oscillations in the natural neighbor's map underscore the limitations of purely geometric interpolation on such a faceted reference (Figure 11). By contrast, the proposed ANN + Blending method leverages learned spatial patterns to produce a smoothly varying surface that respects the measured data while filling gaps in a more physically plausible way. In other words, the "fuzzy" difference patterns for the ANN model are not only small in magnitude, but also suggest that our model adheres to actual topographic continuity better than a rigid triangulated mesh can.

From a broader perspective, these findings reinforce the benefits of data-driven smoothing techniques in complex topographies. Classical interpolation algorithms (e.g. TIN, IDW, splines) are model-driven – they impose predetermined shapes between points (planar facets or weighted averages) which can lead to artifacts if the terrain is highly irregular or sparsely sampled (Gold and Dakowicz, 2002; Kobler et al., 2007). This often necessitates manual intervention to fix issues like spikes, pits or unnatural breaks in the generated surface. Machine-learning approaches, on the other hand, offer an adaptive framework that can learn the nonlinear relationships inherent in terrain data (Procopio et al., 2009). In our case, the ANN was trained to capture how elevation varies with different spatial configurations of neighboring points, essentially internalizing typical landform behaviors. As with the Topographically InformEd Regression (TIER) model (Newman and Clark, 2020), which incorporates terrain attributes into its regression-based interpolation, our approach ensures that local landform features are explicitly considered in surface generation, thus improving the physical realism of the final terrain model. The result is an interpolated surface that naturally smooths out noise and spurious fluctuations while retaining genuine terrain features. Notably, the blending strategy further enhances surface continuity and stability – by aggregating multiple ANN outputs, the model likely cancels out any outlier predictions and avoids over-fitting to local anomalies. This concept of combining models or data sources to offset individual weaknesses has precedent in DEM research; for instance, fusing multiple elevation data types via neural networks has been shown to yield higher-quality models than any single source alone (Kumar Arora and Mathur, 2001). Our approach aligns with this philosophy, effectively integrating a learned component into the interpolation process to harness the strengths of both data-driven learning and traditional surface modeling.

A key outcome of the study is the high accuracy achieved by the proposed method even in a large, topographically complex area, without the need for manual post-editing. In the most extensive test region (Hasanbey, ~31,630 m²), the ANN + Blending model attained a mean squared error of only 4.116×10^{-5} with respect to the reference – an extremely low error considering the size and complexity of this terrain. Crucially, this performance was obtained through a fully automated process. Generating a high-fidelity DTM for such challenging terrain using conventional means typically demands substantial expert effort: practitioners must identify and correct interpolation artifacts, enforce terrain breaklines, or fine-tune parameters to handle steep or irregular features. Such manual editing is not only time-consuming but can introduce subjective biases. The fact that our learning-based model produces an accurate surface out-of-the-box, without any hand-

https://doi.org/10.5194/egusphere-2025-2539
Preprint. Discussion started: 1 September 2025

tuning for the Hasanbey site, underscores a major advantage. It demonstrates robustness and generalizability – the model effectively "adapts" to different landscape characteristics on its own.

This level of automation addresses an oft-cited challenge in DTM production: the need for methods that yield high accuracy with minimal human intervention. Our findings resonate with the observations of Parquer et al. (2025), who emphasize that even when numerical or algorithmic consistency is achieved in 3D models, domain expertise is still required to ensure their practical validity for downstream applications. By drastically reducing the manual workload, our approach can improve the efficiency and consistency of terrain modeling in practice, while also reducing the potential for human-induced errors or inconsistencies.

In summary, the proposed ANN + Blending method bridges the gap between the rigidity of traditional models and the adaptability of modern, learning-based interpolation. Conventional TIN or spline models, while mathematically straightforward and exact at given data points, lack the flexibility to gracefully accommodate complex, unseen terrain variations – they often enforce a rigid structure that either misses subtleties or requires laborious post-corrections (Li and Kuai, 2014). Our approach marries this classical reliability with the intelligence of machine learning: it respects measured elevations and known terrain structure (as a TIN would) but also generalizes the surface in a data-informed way to ensure natural continuity. The outcome is a terrain model that achieves the best of both worlds – high fidelity to observed data and smooth adaptability to the landscape's intricacies. This finding is in line with recent views in the literature that call for hybrid solutions blending interpolation with intelligent modeling to surpass the limitations of either alone. Overall, the ANN + Blending technique represents a significant step toward more accurate and automated DTM generation. It provides a robust solution that can handle large and complex topographies, maintaining terrain realism without sacrificing precision or requiring intensive user oversight. Such a balance between accuracy, continuity, and automation is highly desirable for next-generation digital terrain modeling in engineering and geospatial applications.

Code availability statement

Supplementary MATLAB scripts for contour map generation and terrain data visualization have been made publicly available on Figshare under CC BY 4.0 license at https://doi.org/10.6084/m9.figshare.29279717.v1 (Akgol and Kara, 2025a). These scripts support the comparative analysis and visualization components of this study.

Data availability statement

Processed coordinate datasets for the three test sites (Alemdar-1, Alemdar-2, and Hasanbey) have been made publicly available on Figshare under CC BY 4.0 license at https://doi.org/10.6084/m9.figshare.29279729.v1 (Akgol and Kara, 2025b). These datasets contain (X, Y, Z) coordinate data that support the evaluation of digital terrain modeling methods presented in this study, enabling reproducibility of the comparative analysis and performance evaluation results.

https://doi.org/10.5194/egusphere-2025-2539
Preprint. Discussion started: 1 September 2025

Author contribution

Kadir Akgol conceived the research idea, designed the methodology, and supervised the study. Yelda Nur Kara conducted the literature review, performed the analyses, and contributed to the interpretation of the results. Both authors contributed to writing and editing the manuscript.

Competing interests

The authors declare that they have no competing interests.

References

Abdel-Aziz, T., Dawod, G., and Ebaid, H.: DEMs and reliable sea level rise risk monitoring in Nile Delta, Egypt, Discover Sustainability, 1, 1-11, 2020.
Akgol, K. and Kara, Y. N.: MATLAB Script for Generating Terrain Contour Maps from XYZ Data, figshare [code], https://doi.org/10.6084/m9.figshare.29279717.v1, 2025a.
Akgol, K. and Kara, Y. N.: GPS-Based Terrain Data for Benchmarking Digital Terrain Modeling Methods, figshare [dataset], https://doi.org/10.6084/m9.figshare.29279729.v1, 2025b.
Alavi, Y., Chartrand, G., Chung, F. R., Erdös, P., Graham, R. L., and Oellermann, O. R.: Highly irregular graphs, Journal of Graph Theory, 11, 235-249, 1987.
Ali, T. and Mehrabian, A.: A novel computational paradigm for creating a Triangular Irregular Network (TIN) from LiDAR data, Nonlinear Analysis: Theory, Methods Applications, 71, e624-e629, 2009.
Arun, P.: A terrain-based hybrid approach towards DEM interpolation, Annals of GIS, 19, 245-252, 2013.
Bandara, K. R., Samarakoon, L., Shrestha, R. P., and Kamiya, Y.: Automated generation of digital terrain model using point clouds of digital surface model in forest area, Remote Sensing, 3, 845-858, 2011.
Baudot, Y.: A comparison of different methods used to generate digital elevation models, [Proceedings] IGARSS'91 Remote Sensing: Global Monitoring for Earth Management, Espoo, Finland, 2435-2438,
Bertram, M. and Hagen, H.: Reducing Interpolation Artifacts by Globally Fairing Contours, in: Mathematical Foundations of Scientific Visualization, Computer Graphics, and Massive Data Exploration, Springer, 257-269, 2009.
Bertram, M., Barnes, J. C., Hamann, B., Joy, K. I., Pottmann, H., and Wushour, D.: Piecewise optimal triangulation for the approximation of scattered data in the plane, Computer Aided Geometric Design, 17, 767-787, 2000.
Besic, N., Picard, N., Vega, C., Bontemps, J. D., Hertzog, L., Renaud, J. P., Fogel, F., Schwartz, M., Pellissier-Tanon, A., Destouet, G., Mortier, F., Planells-Rodriguez, M., and Ciais, P.: Remote-sensing-based forest canopy height mapping: some models are useful, but might they provide us with even more insights when combined?, Geosci. Model Dev., 18, 337-359, 10.5194/gmd-18-337-2025, 2025.
Çubukçu, E. A., Demir, V., and Sevimli, M. F.: Digital elevation modeling using artificial neural networks, deterministic and geostatistical interpolation methods, Turkish Journal of Engineering, 6, 199-205, 2022.
Darnell, A. R., Lovett, A. A., Barclay, J., and Herd, R. A.: An application-driven approach to terrain model construction, International Journal of Geographical Information Science, 24, 1171-1191, https://doi.org/10.1080/13658810903318889, 2010.
Didona, D. and Romano, P.: Hybrid machine learning/analytical models for performance prediction: A tutorial, ICPE '15: Proceedings of the 6th ACM/SPEC International Conference on Performance Engineering, Texas, Austin, USA, 341-344,
Eurich, C. W. and Schulzke, E. L.: Irregular connectivity in neural layers yields temporally stable activity patterns, Neurocomputing, 58, 979-984, 2004.
Fan, L., Smethurst, J., Atkinson, P., and Powrie, W.: Propagation of vertical and horizontal source data errors into a TIN with linear interpolation, International journal of geographical information science, 28, 1378-1400, 2014.

https://doi.org/10.5194/egusphere-2025-2539
Preprint. Discussion started: 1 September 2025

Florinsky, I. V.: Errors of signal processing in digital terrain modelling, International Journal of Geographical Information Science, 16, 475-501, 2002.
Fritsch, D., Hahn, M., and Schneider, F.: Automatic DTM generation from MOMS-O2/D2 mode 1 data, Remote Sensing and Reconstruction for Three-Dimensional Objects and Scenes, San Diego, CA, United States, 20-27,
Gold, C. and Dakowicz, M.: Terrain modelling based on contours and slopes, 10th International Symposium on Spatial Data Handling (SDH), Ottawa, Canada, Jul 09-12, WOS:000177780200008, 95-107, 2002.
Gui, R., Qin, Y., Hu, Z., Dong, J., Sun, Q., Hu, J., Yuan, Y., and Mo, Z.: Neural Network-Based Fusion of InSAR and Optical Digital Elevation Models with Consideration of Local Terrain Features, Remote Sensing, 16, 3567, 2024.
Heimsath, A. M. and Farid, H.: Hillslope topography from unconstrained photographs, Mathematical Geology, 34, 929-952, 2002.
Hu, Y. and Tao, C. V.: Hierarchical recovery of digital terrain models from single and multiple return lidar data, Photogrammetric Engineering Remote Sensing, 71, 425-433, 2005.
Jiang, J., Liu, S., and Yan, H.: Algorithm Designing and Realizing of TIN in VB, Surveying Mapping, 29, 64-67, 2006.
Jiang, W. and Xie, J.: TIN based image segmentation for man-made feature extraction, MIPPR 2005: Image Analysis Techniques, 396-402,
Jiao, L. and Liu, Y.: DEM interpolation based on artificial neural networks, MIPPR 2005: Geospatial Information, Data Mining, and Applications, Wuhan, China, 663-673,
Kobler, A., Pfeifer, N., Ogrinc, P., Todorovski, L., Oštir, K., and Džeroski, S.: Repetitive interpolation: A robust algorithm for DTM generation from Aerial Laser Scanner Data in forested terrain, Remote Sensing of Environment, 108, 9-23, 2007.
Kumar Arora, M. and Mathur, S.: Multi-source classification using artificial neural network in a rugged terrain, Geocarto International, 16, 37-44, 2001.
Li, L. and Kuai, X.: An efficient dichotomizing interpolation algorithm for the refinement of TIN-based terrain surface from contour maps, Computers Geosciences, 72, 105-121, 2014.
Li, R., Sun, T., Tian, F., and Ni, G. H.: SHAFTS (v2022.3): a deep-learning-based Python package for simultaneous extraction of building height and footprint from sentinel imagery, Geosci. Model Dev., 16, 751-778, 10.5194/gmd-16-751-2023, 2023.
Li, R., Tang, Z., Li, X., and Winter, J.: Drainage structure datasets and effects on LiDAR-Derived surface flow modeling, ISPRS International Journal of Geo-Information, 2, 1136-1152, 2013.
Lindsay, J. B.: Efficient hybrid breaching-filling sink removal methods for flow path enforcement in digital elevation models, Hydrological Processes, 30, 846-857, 2016.
Magillo, P., De Floriani, L., and Iuricich, F.: Morphologically-aware elimination of flat edges from a TIN, Proceedings of the 21st ACM SIGSPATIAL International Conference on Advances in Geographic Information Systems, 244-253,
Mesa-Mingorance, J. L. and Ariza-López, F. J.: Accuracy assessment of digital elevation models (DEMs): A critical review of practices of the past three decades, Remote Sensing, 12, 2630, 2020.
Narendran, J., Srinivas, P., Udayalakshmi, M., and Muralikrishnan, S.: Quality Metrics of Semi Automatic DTM from Large Format Digital Camera, The International Archives of the Photogrammetry, Remote Sensing Spatial Information Sciences, 40, 1159-1163, 2014.
Newman, A. J. and Clark, M. P.: TIER version 1.0: an open-source Topographically InformEd Regression (TIER) model to estimate spatial meteorological fields, Geosci. Model Dev., 13, 1827-1843, 10.5194/gmd-13-1827-2020, 2020.
Parquer, M. N., de Kemp, E. A., Brodaric, B., and Hillier, M. J.: Checking the consistency of 3D geological models, Geosci. Model Dev., 18, 71-100, 10.5194/gmd-18-71-2025, 2025.
Procopio, M. J., Kegelmeyer, W. P., Grudic, G., and Mulligan, J.: Terrain Segmentation with On-Line Mixtures of Experts for Autonomous Robot Navigation, 8th International Workshop on Multiple Classifier Systems, Univ Iceland, Reykjavik, ICELAND, Jun 10-12, WOS:000269293000039, 385-+, 2009.
Rana, S.: Use of plan curvature variations for the identification of ridges and channels on DEM, Progress in Spatial Data Handling: 12th International Symposium on Spatial Data Handling, Berlin, Heidelberg, 789-804,
Rebecca, O. and Gold, C.: TIN meets CAD—extending the TIN concept in GIS, Future Generation Computer Systems, 20, 1171-1184, 2004.
Sakhaee, E. and Entezari, A.: Spline-based Sparse Tomographic Reconstruction with Besov Priors, Conference on Medical Imaging - Image Processing, Orlando, FL, Feb 24-26, WOS:000355653800013, 10.1117/12.2082797, 2015.

https://doi.org/10.5194/egusphere-2025-2539
Preprint. Discussion started: 1 September 2025

Stupariu, M.-S.: Discrete curvatures of triangle meshes: From approximation of smooth surfaces to digital terrain data, Computers Geosciences, 153, 104789, 2021.

Van Kreveld, M.: Digital elevation models and TIN algorithms, in: Algorithmic Foundations of Geographic Information Systems, Springer, Berlin, Heidelberg, 37-78, 1996.

Zhang, X., Zeng, Q., Jiao, J., and Zhang, J.: Fusion of space-borne multi-baseline and multi-frequency interferometric results based on extended Kalman filter to generate high quality DEMs, ISPRS journal of photogrammetry remote sensing, 111, 32-44, 2016.